Electrophysiology and staining. Recording electrodes were glass micropipettes filled with 2–4% biocytin (Sigma) dissolved in 1 M potassium acetate. Electrode resistances ranged from 30 to 100 MΩ. The recording electrodes were aligned so that the tips would meet approximately 1–2 mm ventral to the dorsal surface of the striatum. After recording electrodes were inserted, the exposed cortex was covered with a low-melting-point paraffin wax to reduce brain pulsations. Recordings were made using an active bridge amplifier and then filtered and digitized at a rate of 4 kHz or higher. Neurons that had membrane potentials more negative than −60 mV and action potentials more positive than 0 mV were included in the sample. Neurons were stained by passing 1.5-nA depolarizing pulses of 300 ms duration every 600 ms for 10–60 min.

Histology. At the end of the experiment, the animals were given a lethal dose of Nembutal or urethane intraperitoneally and were perfused intracardially with isotonic buffered saline followed by 400 ml of 4% formaldehyde in 0.15 M sodium phosphate buffer (pH 7.2–7.6). Intact brains were removed and postfixed in cold phosphate-buffered formaldehyde. The brains were trimmed and cut on a vibratome in 50-μm parasagittal sections. Sections containing labelled neurons or processes were processed for biocytin[30]. Some sections were postfixed with 1% osmium tetroxide. Cells were identified by the coordinates of the recording electrodes, which were recorded during the experiment. Only pairs in which both neurons were identified were used in the sample.

Data analysis. The membrane potential distribution was normalized and the weighted sum of two gaussians was fit to the data using the Levenberg–Marquart method of nonlinear least squares. The model used was

$$p(v) = \frac{a}{\sqrt{2\pi}\sigma_1}\exp\left(\frac{(v-\mu_1)}{2\sigma_1^2}\right) + \frac{1-a}{\sqrt{2\pi}\sigma_2}\exp\left(\frac{(v-\mu_1)}{2\sigma_2^2}\right)$$

where μ_1 is the mean membrane potential in the 'down' state; σ_1 is the amplitude of fluctuations within the 'down' state; μ_2 is the mean membrane potential in the 'up' state; σ_1 is the amplitude of fluctuations within the 'up' state and a is the ratio of 'down' state to 'up' state. After the two best-fitting gaussians were found, we defined the thresholds of the 'up' and 'down' states as half of the distance between the minimum point between the two gaussians and the modal point for that state. Using these methods, the state transition times were converted into a point process, which was used to construct the auto- and cross-correlograms of the state transitions. Cross-correlograms were constructed from the transition times of the two states, rather than cross-correlating the waveforms of the membrane potential, so that the only contribution to the central peak would be the jitter in the delay between the two neurons' membrane-potential transition times. Cross-correlating the membrane-potential waveforms would result in a broader peak owing to the variability of the autocorrelation waveforms, that is, the durations of the 'up' and 'down' states in each cell. Auto- and cross-correlograms of state transitions and spikes were calculated using standard methods[16] implemented using the program Mathematica. All cross-correlograms were compared to autocorrelograms of the component neurons. The central peak in the cross-correlogram, which was present for each cell pair, was never present in the autocorrelograms. Synchrony (strength of cross-correlation) was calculated by dividing the magnitude of the central peak by the standard deviation of the correlogram. Cross-correlation of the waveforms was performed using standard time-series methods[13] implemented in Mathematica. The cross-correlations were calculated starting from 100 ms from the first peak within the 'up' state. Only 'up' states without spikes were selected. 95% confidence intervals were calculated for the harmonic means of 6 cross-correlations.

Received 9 March; accepted 8 June 1998.

1. Graybiel, A. M., Aosaki, T., Flaherty, A. W. & Kimura, M. The basal ganglia and adaptive motor control. *Science* **265,** 1826–1831 (1994).
2. Wilson, C. J. in *The Synaptic Organization of the Brain* (ed. Shepherd, G.) 329–375 (Oxford Univ. Press, New York, 1997).
3. Wilson, C. J. & Groves, P. M. Spontaneous firing patterns of identified spiny neurons in the rat neostriatum. *Brain Res.* **220,** 67–80 (1981).
4. Wilson, C. J. & Kawaguchi, Y. The origins of two-state spontaneous membrane potential fluctuations of neostriatal spiny neurons. *J. Neurosci.* **16,** 2397–2410 (1996).
5. Stern, E. A., Kincaid, A. E. & Wilson, C. J. Spontaneous subthreshold membrane potential fluctuations and action potential variability of rat corticostriatal and striatal neurons in vivo. *J. Neurophysiol.* **77,** 1697–1715 (1997).
6. Wickens, J. R. & Wilson, C. J. Regulation of action potential firing in spiny neurons of the rat neostriatum in vivo. *J. Neurophysiol.* **79,** 2358–2364 (1998).
7. Choi, S. & Lovinger, D. M. Decreased frequency but not amplitude of quantal synaptic responses associated with expression of corticostriatal long-term depression. *J. Neurosci.* **17,** 8613–8620 (1997).
8. Wilson, C. J. in *Single Neuron Computation* (eds McKenna, T., Davis, J. & Zornetzer, S. F.) 141–171 (Academic, San Diego, 1992).
9. Alexander, G. E. & DeLong, M. R. Microstimulation of the primate neostriatum. I. Physiological properties of striatal microexcitable zones. *J. Neurophysiol.* **53,** 1401–1416 (1985).
10. Flaherty, A. W. & Graybiel, A. M. Two input systems for body representations in the primate striatal matrix: Experimental evidence in the squirrel monkey. *J. Neurosci.* **13,** 1120–1137 (1993).
11. Alexander, G. E. & DeLong, M. R. Microstimulation of the primate neostriatum. II. Somatotopic organization of striatal microexcitable zones and their relation to neuronal response properties. *J. Neurophysiol.* **53,** 1417–1430 (1985).
12. Jaeger, D., Gilman, S. & Aldridge, J. W. Neuronal activity in the striatum and palladium of primates related to the execution of externally cued reaching movements. *Brain Res.* **694,** 11–127 (1995).
13. Diggle, P. *Time Series* (Oxford Univ. Press, 1990).
14. Abeles, M. Quantification, smoothing, and confidence limits for single-units' histograms. *J. Neurosci. Methods* **5,** 317–325 (1982).
15. Wilson, C. J. Postsynaptic potentials evoked in spiny neostriatal projection neurons by stimulation of ipsilateral and contralateral cortex. *Brain Res.* **367,** 201–213 (1986).
16. Perkel, D. H., Gerstein, G. L. & Moore, G. P. Neuronal spike trains and stochastic point processes. *Biophys. J.* **7,** 419–440 (1967).
17. Onn, S. P. & Grace, A. A. Dye coupling between rat striatal neurons recorded in vivo: compartmental organization and modulation by dopamine. *J. Neurophysiol.* **71,** 1917–1934 (1994).
18. Jaeger, D., Kita, H. & Wilson, C. J. Surround inhibition among projection neurons in weak or nonexistent in the rat neostriatum. *J. Neurophysiol.* **72,** 2555–2558 (1994).
19. Steriade, M., Nunez, A. & Amzica, F. A novel slow (<1 Hz) oscillation of neocortical neurons in vivo: depolarizing and hyperpolarizing components. *J. Neurosci.* **13,** 3252–3265 (1993).
20. Amzica, F. & Steriade, M. Short- and long-range neuronal synchronization of the slow (<1 Hz) cortical oscillation. *J. Neurophysiol.* **73,** 20–38 (1995).
21. Contreras, D. & Steriade, M. State-dependent fluctuations of low-frequency rhythms in corticothalamic rhythms. *Neuroscience* **76,** 25–38 (1995).
22. Douglas, R. J., Martin, K. A. C. & Whitteridge, D. An intracellular analysis of the visual responses of neurons in cat visual cortex. *J. Physiol. (Lond.)* **440,** 659–696 (1991).
23. Wilson, C. J. The generation of natural firing patterns in neostriatal neurons. *Prog. Brain Res.* **99,** 277–297 (1993).
24. Hull, C. D., Bernardi, G. & Buchwald, N. A. Intracellular responses of caudate neurons to brain stem stimulation. *Brain Res.* **22,** 163 (1970).
25. Plenz, D. & Kitai, S. T. Up and down states in striatal medium spiny neurons simultaneously recorded with spontaneous activity in fast-spiking interneurons studied in cortex-striatum-substantia nigra organotypic cultures. *J. Neurosci.* **18,** 266–283 (1998).
26. Stern, E. A., Aertsen, A., Vaadia, E. & Hochstein, S. Stimulus encoding by multidimensional receptive fields in single cells and cell populations in V1 of awake monkey. *Adv. Neural Inf. Process. Systems* **5,** 377 (1993).
27. Arieli, A., Sterkin, A., Grinvald, A. & Aertsen, A. Dynamics of ongoing activity: explanation of the large variability in evoked cortical responses. *Science* **273,** 1868–1871 (1996).
28. O'Keefe, J. & Reece, M. L. Phase relationship between hippocampal place units and the EEG theta rhythm. *Hippocampus* **3,** 317–330 (1993).
29. Skaggs, W. E., McNaughton, B. L., Wilson, M. A. & Barnes, C. A. Theta phase precession in hippocampal neuronal populations and the compression of temporal sequences. *Hippocampus* **6,** 149–172 (1996).
30. Horikawa, K. & Armstrong, W. E. A versatile means of intracellular labeling: injection of biocytin and its detection with avidin conjugates. *J. Neurosci. Methods* **25,** 1–11 (1988).

Acknowledgements. This work was supported by a grant from the NIH. We thank B. Mattix for technical assistance.

Correspondence and requests for materials should be addressed to E.S. (edstern@marlin.utmem.edu).

Glutamate locally activates dendritic outputs of thalamic interneurons

Charles L. Cox, Qiang Zhou & S. Murray Sherman

Department of Neurobiology, State University of New York, Stony Brook, New York 11794-5230, USA

The relay of information through thalamus to cortex is dynamically gated, as illustrated by the retinogeniculocortical pathway[1]. Important to this is the inhibitory interneuron in the lateral geniculate nucleus (LGN). For the typical neuron, synaptic information arrives through postsynaptic dendrites and is transmitted by axon terminals. However, the typical thalamic interneuron, in addition to conventional axonal outputs, has distal dendrites that serve both pre- and postsynaptic roles[2–6]. These dendritic terminals participate in curious and enigmatic triadic arrangements, in which each contacts a relay cell dendrite and is contacted by a glutamatergic retinal terminal that innervates the same relay cell dendrite. Here we show that agonists of the metabotropic glutamate receptor (mGluR) activate dendritic terminals of interneurons in the absence of action potentials, thereby inhibiting the postsynaptic relay neuron. Somatic recordings from LGN interneurons reveal that there is no response to mGluR agonists, suggesting that their dendritic terminals are electrically isolated

from their somata and axons, consistent with anatomical modelling of these cells[7]. Our results offer insight into the functioning of triadic circuitry and indicate that thalamic interneurons can perform independent computations expressed through axonal as opposed to dendritic outputs.

Local, GABAergic, inhibitory inputs to dendrites of relay cells of the LGN derive from three sources: two are axonal—from interneurons and neurons in the thalamic reticular nucleus (TRN)—and the other is from the dendritic terminals of interneurons (see also below). The axonal terminals, also known as F1 terminals, are presynaptic only, and form conventional inhibitory synaptic contacts. The dendrites of the interneurons have been described as "axoniform"[8], because at their distal regions they give rise to small, thin stalks terminating in dendritic terminals. These are known as F2 terminals, and they are unusual in that they are both pre- and postsynaptic (reviewed in ref. 1; Fig. 1A). These F2 terminals are usually involved in triads (Fig. 1A, shaded area), in which the retinogeniculate terminal provides excitatory contacts onto both a relay cell dendrite and the F2 terminal, with the F2 terminal contacting the same relay cell dendrite (Fig. 1A). This arrangement suggests that the retinal input produces both monosynaptic excitation and feedforward disynaptic inhibition at the relay cell. Finally, although all LGN relay cells receive inputs from F1 terminals, only morphological type 2 cells (thought to be X; see refs 9, 10) receive significant numbers of F2 inputs[11], and type 1 cells (thought to be Y) do not; thus, only type 2 cells should display physiology reflecting triadic inputs involving F2 terminals[11]. The problem has been to test the function of these triadic circuits, which have previously been defined anatomically but not physiologically because of the difficulty in recording from or selectively activating the F2 terminals.

A possible solution to this problem was offered by immunocytochemical studies of the distribution of mGluRs in the cat's LGN[12], which indicated that mGluRs are selectively located postsynaptic to cortical inputs on relay cell dendrites and on F2 terminals postsynaptic to retinal input. By suppressing the postsynaptic actions of mGluR activation in the relay neurons, this arrangement allows the possibility of selectively stimulating F2 terminals with mGluR agonists, thereby gaining a glimpse into the functioning of these terminals specifically and interneurons more generally. We did this by using whole-cell recording of relay cells and interneurons from *in vitro* thalamic slice preparations of cats and rats.

During current clamp recording of cat LGN relay cells, the general mGluR agonist (±)-1-aminocyclopentane-*trans*-1,3-dicarboxylic acid (ACPD) produced a long-lasting membrane depolarization associated with an increased input resistance (Fig. 1B). This presumably acts through the mGluRs on relay cell dendrites and is consistent with previous demonstrations that mGluR activation reduces a resting potassium 'leak' conductance (K_{leak}), thereby depolarizing the membrane[13,14]. We also noticed that ACPD application produced a large increase in the baseline activity (Fig. 1Bb) that persisted independently of the ACPD-mediated membrane depolarization (Fig. 1Bc) and was suppressed by the $GABA_A$ antagonist bicuculline methiodid (BMI; data not shown). We conclude that this increased activity reflected spontaneous inhibitory postsynaptic potentials (sIPSPs), which also implies that this effect is independent of the ACPD-mediated reduction of K_{leak} in the postsynaptic neuron.

To help isolate spontaneous inhibitory postsynaptic currents (sIPSCs), we minimized the effect of ACPD on K_{leak} by substituting Cs^+ for K^+ in the recording pipette (Cs^+ will thus diffuse into the cell and block the K^+ conductance underlying K_{leak}), and we made voltage clamp recordings with a holding potential of 0 mV to increase the driving force of the presumed Cl^- conductance (Fig. 1C, D). Under these conditions, application of ACPD (125–250 μM) increased the amplitude and frequency of sIPSCs ($n = 19$ cells; Fig. 1C). These sIPSCs were eliminated or strongly attenuated by BMI (30 μM; $n = 8$ of 8 cells tested; Fig. 2Ad), and their reversal potential was near the calculated Cl^- equilibrium potential (data not shown). This further supports the conclusion that these sIPSCs activated by ACPD application represented activation of $GABA_A$ receptors.

One explanation for the increased sIPSC activity is that ACPD activated local inhibitory neurons (TRN cells and/or interneurons) that form synaptic contacts through F1 terminals onto the recorded neurons (Fig. 3A). To eliminate this possibility, we applied

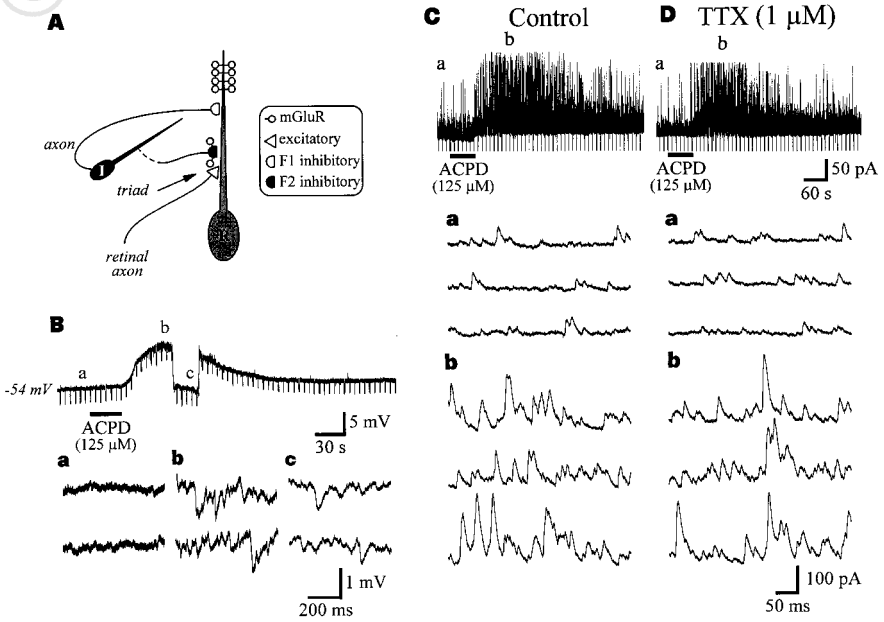

Figure 1 Activation of mGluRs increases inhibition in cat LGN relay neurons. **A**, The retinal axon forms excitatory synapses onto both the relay cell (R) dendrite and the interneuron's (I) F2 terminals. F2 terminals emanate from distal dendrites after many branches (dashed portion) and synapse onto the relay cell. **B**, Current clamp recording from relay cell. ACPD produces a long-lasting depolarization and an increase in baseline activity. The expanded traces (**a**, **b**, **c**) show the baseline activity during the indicated periods. Downward deflections are responses to constant current pulses used to estimate input resistance. **C**, **D**, Voltage clamp recording from relay neuron, **C**, ACPD produces a long-lasting increase in sIPSC activity, as shown in **a**, **b** and then expanded traces below. **D**, This ACPD-mediated increase in sIPSC activity persists in TTX, as shown in **a**, **b**.

tetrodotoxin (TTX) to prevent these inhibitory cells from producing action potentials that could be conducted down their axons to inhibit the recorded relay cells. In 7 of 19 neurons tested, TTX eliminated the ACPD-induced increase in sIPSC activity, suggesting that in these 7 cells the evoked inhibition could be completely explained on the basis of ACPD activation of TRN cells or interneurons. Previous evidence[15], which we confirm here, indicates that interneurons do not respond with increased firing rates to ACPD. However, TRN cells appear to have abundant mGluRs[12] and ACPD application strongly increases their firing rate[16,17]. Thus, the TTX-dependent increase in IPSCs we observed for the 7 cells probably involved an induced increase in activity of TRN inputs to these relay cells.

Surprisingly, the robust increase in sIPSC activity persisted in the presence of TTX in the remaining 12 relay cells (Fig. 1D). In most of these cells, the ACPD effect was slightly attenuated by TTX, suggesting that these neurons contained a TTX-sensitive component of this increased sIPSC activity. As already noted, TTX application eliminates inputs to the relay cell from axonal F1 terminals, which require action potentials for activation, but presumably has little effect on F2 terminals, implying that they do not require action potentials to become activated. If so, then 7 of the recorded cells received synaptic inputs from F1 terminals but from virtually no F2 terminals, as expected for type 1 cells (see above); the remaining 12 cells received inputs from both F1 and F2 terminals, as expected for type 2 cells.

To determine whether the remaining, TTX-insensitive, increase in sIPSC activity resulted from mGluR-evoked GABA release from presynaptic terminals (for example, the F2 terminals) or by an as-yet unidentified postsynaptic effect, we repeated some of these experiments in a low Ca^{2+} (0.2 mM) and high Mg^{2+} (6 mM) extracellular solution. This should eliminate sIPSCs evoked by synaptic transmission, which is Ca^{2+}-dependent. Under these conditions, the TTX-insensitive ACPD-mediated effect was completely suppressed (Fig. 2Aa–c). As an additional control, the amplitudes of the Ca^{2+}-independent miniature IPSCs were not altered by ACPD, indicating the lack of a postsynaptic site of the mGluR-mediated effect in the relay neuron. We conclude that mGluR activation leads to increased GABA release from synaptic terminals, resulting in increased activity of sIPSCs in the recorded relay cells.

From these data alone, we could not determine whether ACPD activates mGluRs directly on axonal (F1) or dendritic (F2) terminals, or both. We therefore took advantage of the unique anatomical organization of the rat thalamus (Fig. 3A). Although the LGN of the rat contains many interneurons and F2 terminals (like that of the cat), the ventrobasal complex (VB) is essentially devoid of

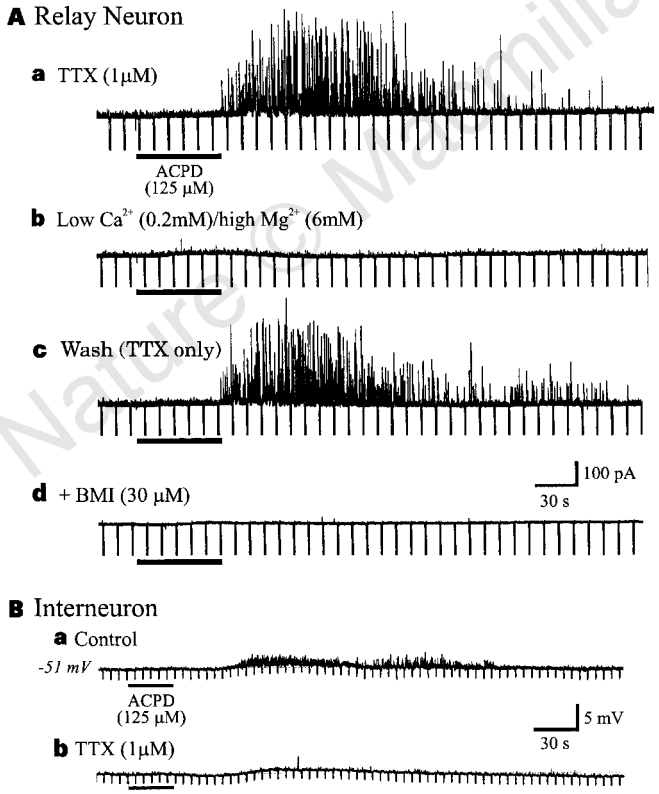

Figure 2 Voltage and current clamp recordings from cat LGN neuron. A, Voltage and current clamp recordings from cat LGN relay neuron demonstrate the synaptic nature of ACPD-mediated increase in sIPSCs. **a**, In TTX, ACPD increases sIPSCs; **b**, in a low-Ca^{2+}/high-Mg^{2+} solution, ACPD produces no change in sIPSC activity; **c**, the ACPD-mediated alteration in sIPSCs recovers following a 20 min wash; **d**, BMI attenuates the sIPSC activity, with and without ACPD. **B**, Current clamp recording from LGN interneuron. **a**, ACPD produces a small, long-latency depolarization (<1 mV) with an increase in sEPSPs. **b**, TTX blocks the increased sEPSPs, but the small depolarization persists.

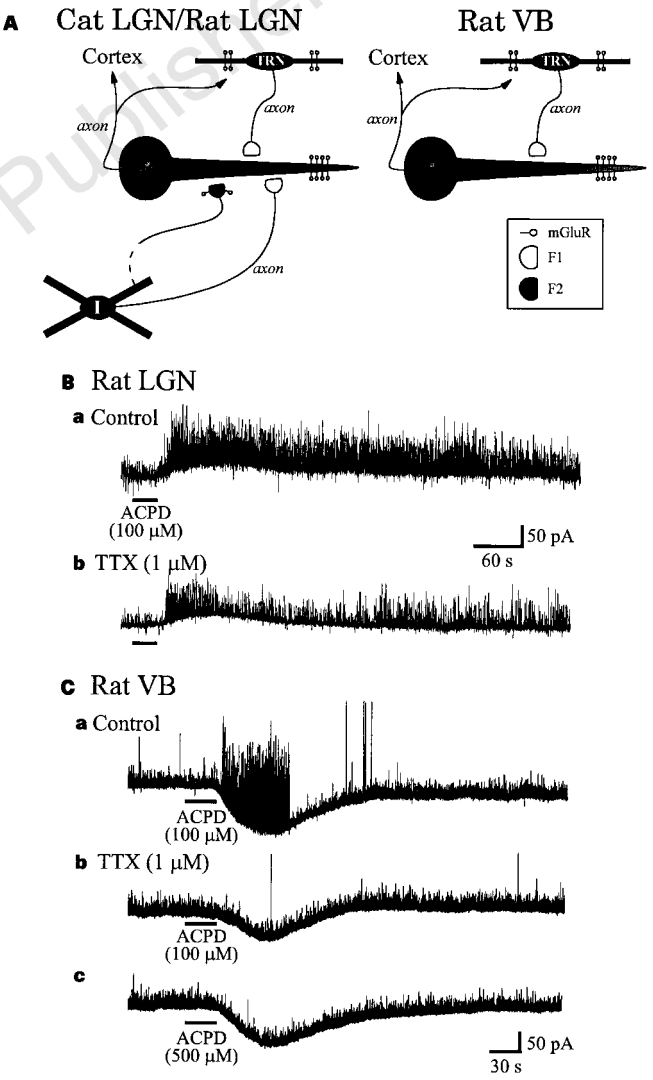

Figure 3 Inhibitory innervation of thalamic relay neurons and voltage clamp recording from rat LGN relay neuron. **A**, Cat LGN/rat LGN: both TRN neurons (TRN) and interneurons (I) contact relay cells (R) via axonal F1 terminals. Dendritic F2 terminals of interneurons also contact relay cells. Rat VB: Rat VB lacks interneurons and F2 terminals, so the relay neuron is inhibited only by F1 terminals. **B**, Voltage clamp recording from rat LGN relay neuron. **a**, ACPD increases sIPSC amplitude and frequency; **b**, in TTX, much of the ACPD-mediated sIPSC increase persists. **C**, Voltage clamp recording from rat VB relay neuron. **a**, ACPD produces a short-lived increase in sIPSCs. **b**, **c**, The ACPD effect is completely blocked in TTX, even with an increased ACPD concentration.

interneurons and F2 terminals[18,19]. Thus IPSCs recorded in rat VB neurons can only result from activation of F1 axonal terminals. In recordings from relay cells of the rat LGN in control conditions, ACPD produced a robust increase in sIPSC activity (Fig. 3Ba; $n = 19$ cells), and this increase persisted in TTX (1 μM) in 5 of 9 cells (Fig. 3Bb). Thus, the TTX-insensitive mGluR effect is present in both rat and cat LGN, nuclei that contain both F1 and F2 terminals.

The effects of ACPD were then tested on rat VB neurons. In control conditions, ACPD increased sIPSC activity in 10 of 17 cells (Fig. 3Ca). However, in contrast to the rat LGN neurons, the ACPD-mediated increase in sIPSC activity was completely suppressed by TTX (1μM) in all nine VB cells tested (Fig. 3Cb, c). These effects of ACPD on rat VB neurons probably represent activation of axons and their F1 terminals from the adjacent TRN. Thus the TTX-insensitive ACPD action was absent in rat VB, a structure containing only F1 terminals, but was present in rat and cat LGNs, each of which contain both F1 and F2 terminals. These results indicate that most or all of the TTX-insensitive increase in sIPSCs we observed in LGN neurons is due to activation of mGluRs on F2 terminals, thereby evoking GABA release and producing inhibitory activity in LGN relay cells.

This conclusion is consistent with immunocytochemical evidence pointing to dense localization of mGluRs on F2 but not F1 terminals in the cat LGN[12]. This, in turn, indicates that interneurons can be activated through mGluRs on the dendritic F2 terminals. However, previous recordings made from somata of interneurons revealed no detectable effects of ACPD[15]. We confirmed this in somatic recordings from four cat LGN interneurons. Interneuron recordings were identified by their characteristic spike discharge properties[15] and two were further identified morphologically, based on injecting biocytin through the recording electrode. ACPD produced no discernible effect on the interneurons except at very long latencies (1–2 min), when there is an increase in spontaneous excitatory post-synaptic potentials (sEPSPs; Fig. 2Ba). In TTX, there remains only a very long latency, small depolarization (Fig. 2Bb). The cause of these curious long-latency effects of ACPD recorded at the somata will require further investigation, but it seems clear that their latency is too long to be related to the effects attributed to activation of the F2 terminals of these same cells (compare Figs 1–3).

Our findings suggest that the effects of activating F2 terminals synaptically (via mGluRs) are so electronically distant from the cell's soma and axon hillock that they have negligible influence there[7]. The interneuron may thus perform simultaneous and largely independent computation operations: one involves inputs to the proximal dendrites and soma expressed conventionally via the axon; the other involves a collection of local functional circuits via F2 terminals that are both pre- and postsynaptic and do not require action potentials. This indicates that the typical somatic recording of these cells may reveal nothing of the processing involving their F2 terminals. In addition, our results offer insight into the functioning of triadic circuitry. The retinal synapses onto relay cells appear to activate only ionotropic glutamate receptors (iGluRs)[14], whereas, as our data indicate, these retinal terminals can activate mGluRs on the F2 terminals. Whether retinal terminals can also activate iGluRs on F2 terminals is not known. Nonetheless, the differential requirements for activation of iGluRs rather than mGluRs suggest that the relative monosynaptic excitation and disynaptic inhibition evoked by retinal inputs in the relay cells may differ with different firing patterns of the retinal axon. For example, mGluR activation may require higher rates of afferent activity than iGluR activation[14], implying that the disynaptic inhibition develops more strongly as the retinal axons fire at a greater frequency. This would limit the amplitude of retinogeniculate transmission more as retinal cells become more excited. This may prevent geniculate relay cells from saturating in their response to stronger visual stimuli, thereby extending their dynamic range of responsiveness to visual stimuli. □

Methods

Slice preparation. Intracellular recordings were made from relay neurons in cat and rat LGN, and rat VB using whole-cell techniques. Thalamic slices were prepared from young cats (5–8 weeks) and rats (postnatal age, 12–18 days) in compliance with approved animal protocols. Briefly, animals were deeply anaesthetized with ketamine (25 mg kg^{-1} for cats; 33 mg kg^{-1} for rats) and pentobarbital sodium (cats only; 50 mg kg^{-1}). A block of tissue containing the LGN and VB was removed and placed in cold, oxygenated slicing solution containing (in mM): 2.5 KCl, 1.25 NaH_2PO_4, 10.0 $MgCl_2$, 0.5 $CaCl_2$, 26 $NaHCO_3$, 11.0 glucose and 234.0 sucrose. Thalamic slices (250–300 μm) were cut in a coronal or sagittal plane with a vibrating tissue slicer and placed in a holding chamber (30 °C) for >2 h before recording. Individual slices were transferred to a submersion-type recording chamber (cat tissue maintained at 30 °C; rat tissue maintained at room temperature) and continuously perfused with oxygenated physiological solution containing (in mM): 126.0 NaCl, 2.5 KCl, 1.25 NaH_2PO_4, 2.0 $MgCl_2$, 2.0 $CaCl_2$, 26.0 $NaHCO_3$, 10.0 glucose, pH 7.4.

Whole-cell recording. Whole-cell recordings were obtained from neurons visualized using a high-power water immersion objective within the slices[20,21]. The recording pipette solution contained (in mM): 117.0 caesium gluconate, 13.0 CsCl, 1.0 $MgCl_2$, 0.07 $CaCl_2$, 0.1 ethylene glycol-*O*,*O*′-bis(2-aminoethyl)-*N*,*N*,*N*′,*N*′-tetraacetic acid (EGTA), 10.0 *N*-(2-hydroxyethyl)piperazine–*N*′-(2-ethanesulphonic acid)(HEPES) and 0.5% biocytin. In some recordings, potassium gluconate and KCl were substituted for Cs gluconate and CsCl. The solutions were adjusted to a final pH of 7.3 and osmolality of 280 mosm. An Axoclamp 2A amplifier (Axon Instruments) was used in continuous single-electrode voltage clamp mode for current recordings. With Cs^+-containing recording pipettes, sIPSCs were recorded in voltage clamp mode at a holding potential (V_{hold}) of 0 mV. Hyperpolarizing voltage steps were repetitively given throughout the experiment to monitor any changes in the access resistance (R_{axs}), and recordings were limited to those cells with a stable $R_{axs} < 20$ MΩ. No correction for liquid junction potential has been made to voltage measurements. ACPD was applied by injecting a bolus into the flow line of the chamber over 30–60 s using a motorized syringe pump. On the basis of the rate of agonist injection and the rate of chamber perfusion, the estimated final bath concentration of ACPD was estimated to be about one-fourth of the concentration introduced in the flow line. All other pharmacological agents were bath-applied.

Received 25 March; accepted 11 May 1998.

1. Sherman, S. M. & Guillery, R. W. Functional organization of thalamocortical relays. *J. Neurophysiol.* **76,** 1367–1395 (1996).
2. Famiglietti, E. V. Jr & Peters, A. The synaptic glomerulus and the intrinsic neuron in the dorsal lateral geniculate nucleus of the cat. *J. Comp. Neurol.* **144,** 285–334 (1972).
3. Guillery, R. W. The organization of synaptic interconnections in the laminae of the dorsal lateral geniculate nucleus of the cat. *Zeitschr. Zellforsch. Mikroskop. Anat.* **96,** 1–38 (1969).
4. Hamos, J. E., Van Horn, S. C., Raczkowski, D., Uhlrich, D. J. & Sherman, S. M. Synaptic connectivity of a local circuit neurone in lateral geniculate nucleus of the cat. *Nature* **317,** 618–621 (1985).
5. Montero, V. M. Localization of gamma-aminobutyric acid (GABA) in type 3 cells and demonstration of their source to F2 terminals in the cat lateral geniculate nucleus: a Golgi–electron-microscopic GABA–immunocytochemical study. *J. Comp. Neurol.* **254,** 228–245 (1986).
6. Ralston, H. J. Evidence for presynaptic dendrites and a proposal for their mechanism of action. *Nature* **230,** 585–587 (1971).
7. Bloomfield, S. A. & Sherman, S. M. Dendritic current flow in relay cells and interneurons of the cat's lateral geniculate nucleus. *Proc. Natl Acad. Sci. USA* **86,** 3911–3914 (1989).
8. Guillery, R. W. A study of Golgi preparations from the dorsal lateral geniculate nucleus of the adult cat. *J. Comp. Neurol.* **128,** 21–50 (1966).
9. Friedlander, M. J., Lin, C.-S., Stanford, L. R. & Sherman, S. M. Morphology of functionally identified neurons in lateral geniculate nucleus of the cat. *J. Neurophysiol.* **46,** 80–129 (1981).
10. LeVay, S. & Ferster, D. Relay cell classes in the lateral geniculate nucleus of the cat and the effects of visual deprivation. *J. Comp. Neurol.* **172,** 563–584 (1977).
11. Wilson, J. R., Friedlander, M. J. & Sherman, S. M. Fine structural morphology of identified X- and Y-cells in the cat's lateral geniculate nucleus. *Proc. R. Soc. B* **22,** 411–436 (1984).
12. Godwin, D. W. *et al.* Ultrastructural localization suggests that retinal and cortical inputs access different metabotropic glutamate receptors in the lateral geniculate nucleus. *J. Neurosci.* **16,** 8181–8192 (1996).
13. Charpak, S., Gähwiler, B. H., Do, K.-Q. & Knöpfel, T. Potassium conductances in hippocampal neurons blocked by excitatory amino-acid transmitters. *Nature* **347,** 765–767 (1990).
14. McCormick, D. A. & von Krosigk, M. Corticothalamic activation modulates thalamic firing through glutamate "metabotropic" receptors. *Proc. Natl Acad. Sci. USA* **89,** 2774–2778 (1992).
15. Pape, H.-C. & McCormick, D. A. Electrophysiological and pharmacological properties of interneurons in the cat dorsal lateral geniculate nucleus. *Neuroscience* **68,** 1105–1125 (1995).
16. Lee, K.H. & McCormick, D. A. Modulation of spindle oscillations by acetylcholine, cholecystokinin and 1*S*,3*R*-ACPD in the ferret lateral geniculate and perigeniculate nuclei *in vitro. Neuroscience* **77,** 335–350 (1997).
17. Sherman, S. M. & Cox, C. L. Excitatory and inhibitory actions of metabotropic glutamate receptor activation in rat thalamic reticular neurons. *Soc. Neurosci. Abstr.* **23,** 73.10 (1997).
18. Arcelli, P., Frassoni, C., Regondi, M. C., De Biasi, S. & Spreafico, R. GABAergic neurons in mammalian thalamus: A marker of thalamic complexity? *Brain Res. Bull.* **42,** 27–37 (1997).

19. Ottersen, O. P. & Storm-Mathisen, J. GABA-containing neurons in the thalamus and protectum of the rodent. An immunocytochemical study. *Anat. Embryol.* **170,** 197–207 (1984).
20. Edwards, F. A., Konnerth, A., Sakmann, B. & Takahashi, T. A thin slice preparation for patch clamp recordings from neurons of the mammalian central nervous system. *Pflugers Arch.* **414,** 600–612 (1989).
21. Stuart, G. J., Dodt, H. U. & Sakmann, B. Patch-clamp recordings from the soma and dendrites of neurons in brain slices using infrared video microscopy. *Eur. J. Physiol.* **423,** 511–518 (1993).

Acknowledgements. This work was supported by National Eye Institute (NIH).

Correspondence and requests for materials should be addressed to S.M.S. (e-mail: ssherman@neurobio.sunysb.edu).

Original antigenic sin impairs cytotoxic T lymphocyte responses to viruses bearing variant epitopes

Paul Klenerman & Rolf M. Zinkernagel

Institute for Experimental Immunology, University Hospital, Schmelzbergstrasse 12, 8091 Zurich, Switzerland

Some viruses, including human immunodeficiency virus (HIV) and hepatitis B virus (HBV) in humans, and lymphocytic choriomeningitis virus (LCMV) in mice, are initially controlled by cytotoxic T lymphocytes (CTLs), but may subsequently escape through mutation of the relevant T-cell epitope[1–3]. Some of these mutations preserve the normal binding to major histocompatibility complex class I molecules, but present an altered surface to the T-cell antigen receptor[4,5]. The exact role of these so-called altered peptide ligands *in vivo* is not clear. Here we report that mice primed with LCMV-WE strain respond to a subsequent infection by WE-derived CTL epitope variants with a CTL response directed against the initial epitope rather than against the new variant epitope. This phenomenon of 'original antigenic sin' was initially described in influenza[6–8] and is an asymmetric pattern of protective antibody crossreactivity determined by exposure to previously existing strains, which may therefore extend to some CTL responses. Original antigenic sin by CTL leads to impaired clearance of variant viruses infecting the same individual and so may enhance the immune escape of mutant viruses evolving in an individual host.

We investigated why many CTL-escape viruses arise and persist, despite an ongoing and apparently intact immune response, by using the murine model of LCMV, a non-cytopathic RNA virus infection in which CTLs are responsible both for the initial control of virus replication and for tissue destruction[9]. CTL responses may select epitope variants that escape recognition in LCMV, HIV or HBV infection[3,10,11]. One such variant virus (LCMV-8.7) arose by selection *in vivo* in C57BL/6 (H–2D^b) mice expressing a transgenic T-cell antigen receptor (TCR)[3]. This has been shown to bear an altered peptide ligand (APL) at the dominant H–2D^b-restricted CTL epitope in the glycoprotein (GP) (33-41: KA**V**YNFATC to KA**L**YNFATC; here described as GP 33-3L). C57BL/6 mice infected with wild-type (WT) LCMV-WE (200 plaque-forming units (PFU) intravenously (i.v.) injected) generated CTLs that partially cross-reacted with the mutant epitope from LCMV-8.7, GP33-3L (Fig. 1a, left panels). Mice primed with LCMV-WE (WT), followed by rechallenge with the same LCMV-WE (WT), likewise had an *ex vivo* response directed primarily against the wild-type epitope (Fig. 1a, middle panels). Surprisingly, secondary challenge with LCMV-8.7 also led to CTLs being primarily specific for the priming epitope, rather than for that of the challenge virus (Fig. 1a, right panels). The asymmetric pattern was the same under two other conditions: when restimulation was performed *in vitro* using specific peptides (Fig. 1b, two left panels) and when priming was done using a recombinant vaccinia virus expressing LCMV-GP (Vac-G2) instead of LCMV itself (Fig. 1b, two right panels). This phenomenon is similar to that described as 'original antigenic sin'—in which antibody responses stimulated by newly arising mutated but serologically related (drifted) influenza strains are predominantly directed against the first strain encountered[7,8]—but this has not been observed previously for T-cell responses *in vivo*.

The same phenomenon was analysed for the major CTL epitope NP118, restricted by L^d or L^q, in which a natural variation between LCMV-WE (RPQ**A**SGVYM; NP118 WT) and LCMV-Docile (RPQ**T**SGVYM; NP118-4T) exists, the latter strain having been derived from a neonatally infected LCMV-WE carrier ICR (L^q) mice[12].

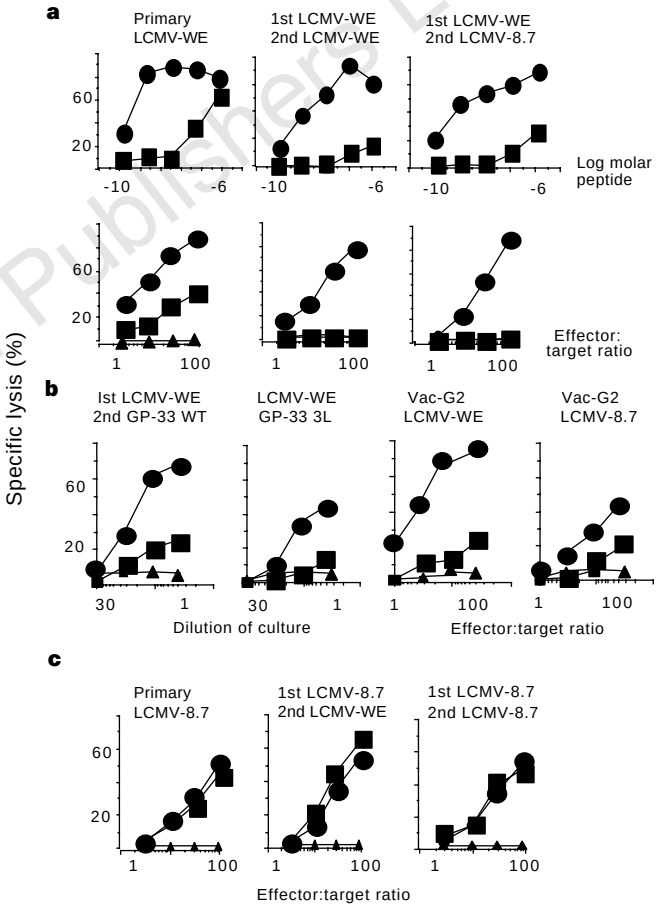

Figure 1 CTL responses of C57BL/6 mice to a single or second virus infection. For all experiments, GP33-WT, GP33-3L and control targets are represented as black circles, squares and triangles respectively. **a**, Primary and secondary responses of C57BL/6 mice to LCMV challenge. Left: mice were infected with LCMV-WE 200 PFU i.v., their splenocytes were collected after 8 days and specific lysis tested against EL4 (H–2D^b) cells sensitized with peptides GP-33 wild type or –3L (upper panels) or against targets prepulsed with peptide at 100 nM (lower panels). Middle and right: C57BL/6 mice were infected with LCMV-WE 200 PFU i.v. and rechallenged with LCMV-WE (middle) or LCMV-8.7 (right). **b**, Responses stimulated with peptide or recombinant vaccinia. Left two panels: splenocytes from C57BL/6 mice previously infected with LCMV-WE were restimulated *in vitro* with GP33-WT (left panel) or 3L variant (right panel) and tested for recognition of peptide-pulsed MC57 targets. Right two panels: the experiment was done as in **a** (middle and right panels) but the initial infection was with Vac-G2 instead of LCMV-WE. **c**, CTL responses of C57BL/6 mice to virus infections in the reverse order (LCMV-8.7 priming). Left: mice were infected with LCMV-8.7 200 PFU i.v., splenocytes were collected after 8 days and specific lysis tested. Middle and right panels: C57BL/6 mice were infected with LCMV-8.7 200 PFU i.v., rechallenged with LCMV-WE or LCMV-8.7 (2×10^6 PFU i.v.) and specific lysis tested.